Dinuclear Metalloradicals

DOI: 10.1002/anie.201203531

Dinuclear Metalloradicals Featuring Unsupported Metal–Metal Bonds**

Edwin F. van der Eide, Ping Yang, Eric D. Walter, Tianbiao Liu, and R. Morris Bullock**

Metal–metal interactions in paramagnetic, multinuclear transition metal complexes are critical to the reactivity of metalloproteins,[1] and understanding them is important in the development of functional metal-containing polymers.[2] Dinuclear mixed-valent complexes—usually obtained by redox reactions[3] of diamagnetic precursors—provide insight into such interactions.[4,5] Bridging ligands are ubiquitous structural motifs in mixed-valent dimers: dithiolate bridges are found in the active site of [FeFe] hydrogenases and models[1] (see $\mathbf{A}^{\bullet+}$, Scheme 1), while bridges formed by unsaturated (hydro)carbon chains and rings,[5] carboxylates,[6] and amidinates[7] are important in other synthetic dimers. Bridging ligands not only mediate the electronic communication[5] between the metal centers; they also provide stabilization against fragmentation. Consequently, much less is known[8] about odd-electron dimers that lack bridges and that are only held together by metal–metal bonds.

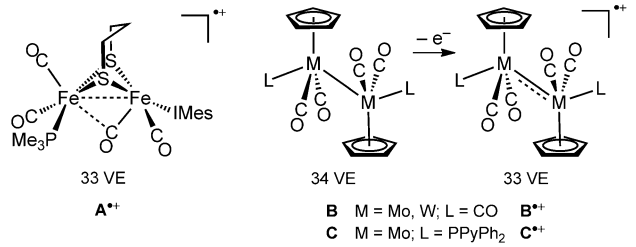

Scheme 1. Are bridging ligands required to stabilize paramagnetic dimers? IMes = 1,3-dimesitylimidazol-2-ylidene, Py = 2-pyridyl, VE = valence electron.

Group 6 dimers $[\{CpM(CO)_3\}_2]$ (**B**, Scheme 1) have unsupported M–M single bonds,[9] and their electrochemistry underscores the need for bridging ligands in stabilizing odd-electron dimers. Electrochemical oxidations of **B** are irreversible due to fast decomposition of $\mathbf{B}^{\bullet+}$ by cleavage of the M–M bond.[10] Derivative $[\{CpMo(CO)_2(PPyPh_2)\}_2]$ (**C**) is reversibly oxidized at low scan rates, but product $\mathbf{C}^{\bullet+}$ is still too short-lived ($t_{1/2} \approx 8$ s)[11] to permit its full characterization. The bonding and spectroscopic properties of these interesting unbridged paramagnetic dimers have thus remained unexplored.[12] Considering that the M–M formal bond order has been proposed to increase from 1 to $1^1/_2$ upon oxidation of **B**, **C**, and other group 6 M^IM^I dimers,[12] we reasoned that stable derivatives of $\mathbf{B}^{\bullet+}$ should be accessible. We report herein the first such derivatives that are stable enough to be isolated and fully characterized.

We attribute the high reactivity of radical cation $\mathbf{B}^{\bullet+}$ largely to its electron poverty—the higher stability of phosphane-containing $\mathbf{C}^{\bullet+}$ confirms this. Hence, usage of the stronger donor phosphane PMe_3 should further increase the lifetime of the radicals. We synthesized $[\{CpW(CO)_2(PMe_3)\}_2]$ (**1**, see Scheme 2)[13] and found that it undergoes an electrochemical oxidation ($E_{1/2} = -0.43$ V vs $[Cp_2Fe]^{\bullet+}/[Cp_2Fe]$, CH_2Cl_2 solvent, 50 mM $nBu_4N^+B(C_6F_5)_4^-$ electrolyte) that remains reversible ($i_c/i_a > 0.9$) at scan rates as low as 50 mV s^{-1}. The separation between the anodic and cathodic peak potentials is 65 mV, indicating that one electron is transferred and that $[\{CpW(CO)_2(PMe_3)\}_2]^{\bullet+}$ ($\mathbf{1}^{\bullet+}$) is the oxidation product. Reversibility of the couple $\mathbf{1}^{\bullet+}/\mathbf{1}$ is maintained when the electrolytes $nBu_4N^+PF_6^-$ or $nBu_4N^+BF_4^-$ (0.1M) are employed, showing that $\mathbf{1}^{\bullet+}$ is (at least on the timescale of the CV experiment) not subject to decomposition by PF_6^- or BF_4^- anions.[14] On a preparative scale, $\mathbf{1}^{\bullet+}$ was synthesized as its $B(C_6F_5)_4^-$ salt[15] by reaction of **1** with 1 equiv $Ph_3C^+B(C_6F_5)_4^-$ in CH_2Cl_2 (Scheme 2). Crystalliza-

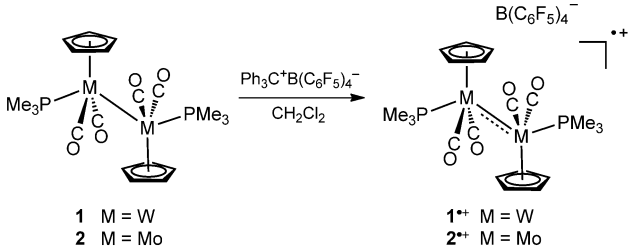

Scheme 2. Synthesis of the dinuclear metalloradicals $\mathbf{1}^{\bullet+}$ and $\mathbf{2}^{\bullet+}$.

[*] Dr. E. F. van der Eide, Dr. T. Liu, Dr. R. M. Bullock
Chemical and Materials Sciences Division
Pacific Northwest National Laboratory
P.O. Box 999, Richland, WA 99352 (USA)
E-mail: morris.bullock@pnnl.gov
Dr. P. Yang, Dr. E. D. Walter
Environmental Molecular Sciences Laboratory
Pacific Northwest National Laboratory
P.O. Box 999, Richland, WA 99352 (USA)
E-mail: ping.yang@pnnl.gov

[**] We thank the U.S. Department of Energy (DOE), Office of Basic Energy Sciences, Division of Chemical Sciences, Geosciences and Biosciences for support of this work. Pacific Northwest National Laboratory (PNNL) is a multiprogram national laboratory operated for DOE by Battelle. The EPR and computational studies were performed using EMSL, a national scientific user facility sponsored by the DOE's Office of Biological and Environmental Research and located at PNNL. We thank Dr. Aaron Appel for useful discussions, and Dr. Charles Windisch for access to his UV/Vis/NIR spectrometer.

Supporting information for this article is available on the WWW under http://dx.doi.org/10.1002/anie.201203531.

tion from CH_2Cl_2/hexanes at room temperature gave $[\mathbf{1}^{\bullet+}]$-$B(C_6F_5)_4^-\cdot{}^1/_2\,CH_2Cl_2$ as analytically pure, air-stable, amber crystals in 90% yield. The dimolybdenum analogue $\mathbf{2}^{\bullet+}$ ($E_{1/2}$ ($\mathbf{2}^{\bullet+}/\mathbf{2}$) = −0.35 V vs $[Cp_2Fe]^+/[Cp_2Fe]$) was similarly accessible, but it was crystallized at −35 °C to prevent decomposition.

Single crystals of **1** and of $[\mathbf{1}^{\bullet+}]B(C_6F_5)_4^-\cdot{}^1/_2\,CH_2Cl_2$ were analyzed[16] by X-ray diffraction (Figure 1, Table 1). The

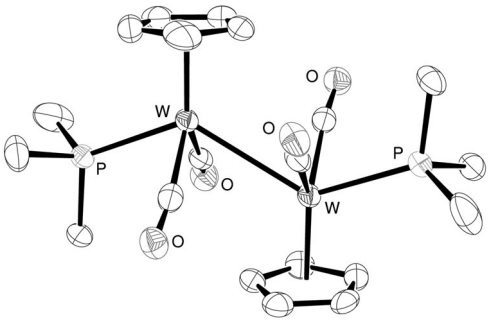

Figure 1. Structure of $[\mathbf{1}^{\bullet+}]B(C_6F_5)_4^-\cdot{}^1/_2\,CH_2Cl_2$ (50% ellipsoids; hydrogen atoms, anion, and solvent omitted).

Table 1: Selected experimental/calculated bond lengths *d* [Å] of **1** and $\mathbf{1}^{\bullet+}$.

	1 [exp][a]	$\mathbf{1}^{\bullet+}$ [exp][b]	**1** [DFT]	$\mathbf{1}^{\bullet+}$ [DFT]
W–W	3.2327(4)	3.0257(3)	3.335	3.127
$(W–P)_{average}$	2.413(1)	2.468(1)	2.437	2.512
$(W–C_{CO})_{average}$	1.950(6)	1.968(6)	1.961	1.976
$(C\equiv O)_{average}$	1.172(7)	1.159(7)	1.186	1.177

[a] C_i symmetry (crystallographically imposed). [b] Near-C_{2h} symmetry.

metric differences between **1** and $\mathbf{1}^{\bullet+}$ are subtle; therefore, only the structure of $\mathbf{1}^{\bullet+}$ is displayed here (see the Supporting Information for a structure overlay). Both dimers assume the *anti* conformation in the solid state and have W–W bonds that are not supported by bridging or semi-bridging[17] carbonyl ligands. The W–W bond length of 3.2327(4) Å in **1** is similar to the length of 3.222(1) Å found in $[\{CpW(CO)_3\}_2]$.[9] The W–W bond length in $\mathbf{1}^{\bullet+}$ is 3.0257(3) Å, corresponding to a significant shortening[18] (6.4%) relative to **1** and strongly suggesting that an increase in the W–W formal bond order occurs upon oxidation.

Density functional (DFT; see the *Experimental Section* for details) calculations provided insight into the electronic structures and aided spectroscopic assignments. The optimized structures of **1** and $\mathbf{1}^{\bullet+}$ are in good agreement with the experimental data (Table 1); the bond-length changes are faithfully reproduced. The MO diagram (Figure 2) clearly shows that the singly occupied MO (SOMO) of $\mathbf{1}^{\bullet+}$, which corresponds to the highest occupied MO (HOMO) of **1**, is antibonding and has π symmetry with respect to the W–W bond. Thus, removal of an electron increases the net W–W formal bond order from 1 (σ) in **1** to $1^1/_2$ ($1\sigma + {}^1/_2\pi$) in $\mathbf{1}^{\bullet+}$. The SOMOs of $\mathbf{1}^{\bullet+}$ and $\mathbf{2}^{\bullet+}$ have largely metal character; spin densities of about 95% (divided equally over both metal centers) are calculated for the M–M cores.

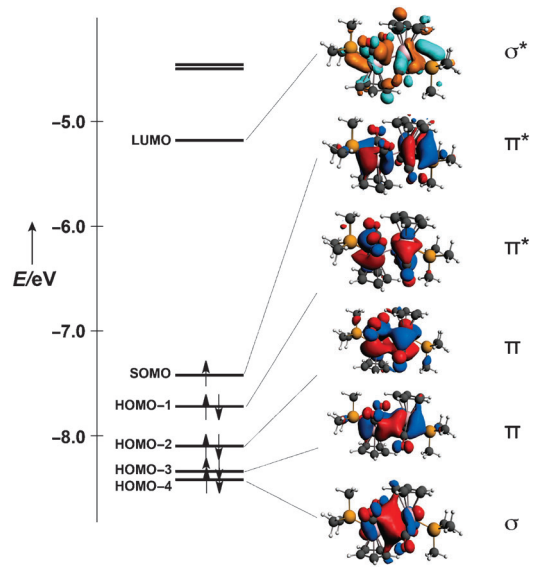

Figure 2. Frontier molecular orbital (MO) energy levels of $\mathbf{1}^{\bullet+}$ and plots of orbitals with metal d character.

The IR spectrum of $\mathbf{1}^{\bullet+}$ in CH_2Cl_2 features one broad carbonyl stretching (ν_{CO}) band at 1875 cm^{-1}.[19] Although two bands (A_u and B_u modes) are expected for a C_{2h}-symmetric species, the small separation of the bands calculated by DFT [(1873 + 1865) cm^{-1}] suggests that they are not resolved experimentally. Precursor **1** has bands at $\tilde{\nu}_{CO}$ = (1837 + 1809) cm^{-1} [DFT: (1840 + 1817) cm^{-1}]. The average $\tilde{\nu}_{CO}$ therefore increases by about 50 cm^{-1} upon oxidation,[20] which correlates well with an increase in the formal oxidation state of each W atom by half a unit.[8,21] The charge (and, therefore, the unpaired electron) in $\mathbf{1}^{\bullet+}$ is shared equally by both W atoms, even on a very short (ps) timescale, in accordance with the calculations. Any contribution from a localized (i.e. W^I–W^{II}) structure can be ruled out.

All of the dimers absorb visible light; the W dimers **1** and $\mathbf{1}^{\bullet+}$ have absorption maxima at λ_{max} = 469 and 434 nm, respectively (Figure 3). Time-dependent DFT predicts these

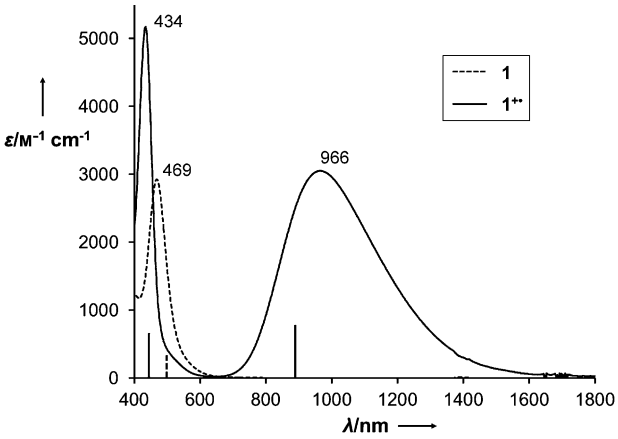

Figure 3. Vis/NIR spectra of **1** and $\mathbf{1}^{\bullet+}$ in CH_2Cl_2. The vertical bars mark the transitions predicted by time-dependent DFT calculations, their heights being proportional to the calculated oscillator strengths.

excitations to occur at 499 and 444 nm, respectively, and allows for their assignment as π*→σ* (see Figure 2, HOMO−1→LUMO).[22] The open-shell dimers also have characteristic near-infrared (NIR) absorptions at $\lambda_{max} = 966$ ($\mathbf{1}^{\bullet+}$, Figure 3) and 1110 nm ($\mathbf{2}^{\bullet+}$). Calculations allow us to assign these as π→π* transitions involving the SOMO (see Figure 2, HOMO−3→SOMO). NIR transitions are characteristic for mixed-valent compounds and are often described as intervalence charge transfers.[23] However, this description implies an electron transfer between metal sites in different oxidation states, which is not applicable to the fully delocalized systems reported herein.

X-band (9.4 GHz) EPR spectra of $\mathbf{1}^{\bullet+}$ and $\mathbf{2}^{\bullet+}$ were recorded in frozen toluene solutions (Figure 4). The spectra

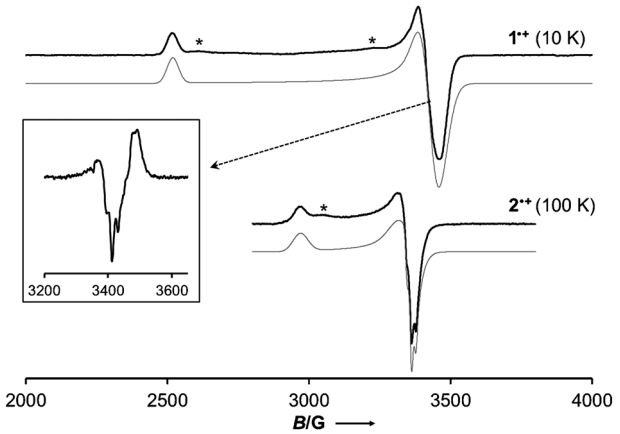

Figure 4. First-derivative-mode EPR spectra in toluene. Simulations in grey. Inset: derivative of the high-field signal of $\mathbf{1}^{\bullet+}$. Resonances marked with an asterisk are assigned to *gauche* isomers.

appear axial as a result of near coincidence of the two lowest principal *g* values. However, simulations and calculations (Table 2) reveal the spectra to be rhombic, as expected for

Table 2: Experimental/calculated EPR parameters of $\mathbf{1}^{\bullet+}$ and $\mathbf{2}^{\bullet+}$.

	$\mathbf{1}^{\bullet+}$ [exp]	$\mathbf{1}^{\bullet+}$ [DFT]	$\mathbf{2}^{\bullet+}$ [exp]	$\mathbf{2}^{\bullet+}$ [DFT]
g_1	2.662	2.606	2.258	2.229
g_2	1.955	1.988	2.002	2.005
g_3	1.940	1.954	1.996	1.996
$A(^{31}P)$[a]	50[b]	43.4[c]	48[b]	42.6[c]

[a] In MHz. [b] Observed in one signal. [c] See the Supporting Information.

species of C_{2h} symmetry. The excellent agreement between calculated and experimental *g* values is noteworthy. The high g_1 values and the large *g* anisotropies ($g_1 - g_3$: 0.72 for $\mathbf{1}^{\bullet+}$; 0.26 for $\mathbf{2}^{\bullet+}$) are good evidence that the spin density is largely metal-based. However, hyperfine coupling to ^{183}W ($I = {}^1/_2$, 14.4 %) or $^{95}Mo/^{97}Mo$ ($I = 5/2$, 25 % total) was not discernible due to line broadening. Coupling to ^{31}P [$I = {}^1/_2$, 100 %, $a_P \approx 17$ G (48 MHz)] is observable in the high-field signal of $\mathbf{2}^{\bullet+}$, and becomes apparent in $\mathbf{1}^{\bullet+}$ when the derivative of the spectrum is shown (Figure 4, inset). The fact that coupling to two equivalent ^{31}P nuclei is observed in both $\mathbf{1}^{\bullet+}$ and $\mathbf{2}^{\bullet+}$ again emphasizes the symmetric delocalization of the unpaired electron over the M−M cores.

In conclusion, our results show that dinuclear metalloradicals with no M−M bridging ligands are not inherently unstable. In fact, oxidation of $[\{CpM(CO)_2(PMe_3)\}_2]$ leads to dinuclear metalloradicals that have additional π bonding between the metal centers. The increased electron density provided by the PMe_3 ligands seems to be crucial in stabilizing the radical cations.

Experimental Section

Synthetic details and characterization data, as well as more complete computational details, are given in the Supporting Information. First-principle calculations based on spin-polarized DFT were performed using the PBE exchange-correlation functional[24] implemented in the Amsterdam Density Functional (ADF 2010.02) program.[25] TZP basis sets with small cores were used for geometry optimization and vibrational frequency analysis; all-electron basis sets were used for property calculations.[26] Scalar relativistic effects were taken into account by the ZORA to the Dirac equation.[27] The time-dependent DFT approach[28] was used to calculate the energies and oscillator strengths of excited states at the optimized ground state geometries. EPR parameters were calculated with inclusion of spin–orbit relativistic effects through the ZORA formalism.[29]

Received: May 8, 2012
Published online: July 23, 2012

Keywords: density functional calculations · EPR spectroscopy · metalloradicals · mixed-valent dimers · redox chemistry

[1] a) M. L. Singleton, N. Bhuvanesh, J. H. Reibenspies, M. Y. Darensbourg, *Angew. Chem.* **2008**, *120*, 9634–9637; *Angew. Chem. Int. Ed.* **2008**, *47*, 9492–9495; b) T. Liu, M. Y. Darensbourg, *J. Am. Chem. Soc.* **2007**, *129*, 7008–7009; c) J. M. Camara, T. B. Rauchfuss, *Nat. Chem.* **2012**, *4*, 26–30; d) A. Jablonskytė, J. A. Wright, S. A. Fairhurst, J. N. T. Peck, S. K. Ibrahim, V. S. Oganesyan, C. J. Pickett, *J. Am. Chem. Soc.* **2011**, *133*, 18606–18609.

[2] M. G. Campbell, D. C. Powers, J. Raynaud, M. J. Graham, P. Xie, E. Lee, T. Ritter, *Nat. Chem.* **2011**, *3*, 949–953.

[3] a) D. Astruc, *Electron Transfer and Radical Processes in Transition-Metal Chemistry*, Wiley-VCH, New York, **1995**; b) N. G. Connelly, W. E. Geiger, *Chem. Rev.* **1996**, *96*, 877–910.

[4] a) M. B. Robin, P. Day, *Adv. Inorg. Chem. Radiochem.* **1967**, *10*, 247–403; b) C. Creutz, H. Taube, *J. Am. Chem. Soc.* **1973**, *95*, 1086–1094; c) K. D. Demadis, C. M. Hartshorn, T. J. Meyer, *Chem. Rev.* **2001**, *101*, 2655–2685.

[5] P. Aguirre-Etcheverry, D. O'Hare, *Chem. Rev.* **2010**, *110*, 4839–4864.

[6] M. H. Chisholm, J. S. D'Acchioli, B. D. Pate, N. J. Patmore, N. S. Dalal, D. J. Zipse, *Inorg. Chem.* **2005**, *44*, 1061–1067.

[7] F. A. Cotton, L. M. Daniels, C. A. Murillo, D. J. Timmons, C. C. Wilkinson, *J. Am. Chem. Soc.* **2002**, *124*, 9249–9256.

[8] The 35 VE species $[\{CpCo(CO)_2\}_2]^{\bullet+}$ is a unique example of a paramagnetic dimer that features an unsupported M−M bond (of order $^1/_2$). Although not isolable, it has been characterized in solution and by DFT: A. Nafady, P. J. Costa, M. J. Calhorda, W. E. Geiger, *J. Am. Chem. Soc.* **2006**, *128*, 16587–16599.

[9] R. D. Adams, D. M. Collins, F. A. Cotton, *Inorg. Chem.* **1974**, *13*, 1086–1090.

[10] K. M. Kadish, D. A. Lacombe, J. E. Anderson, *Inorg. Chem.* **1986**, *25*, 2246–2250.

[11] C. G. Arena, F. Faraone, M. Fochi, M. Lanfranchi, C. Mealli, R. Seeber, A. Tiripicchio, *J. Chem. Soc. Dalton Trans.* **1992**, 1847 – 1853.
[12] Only phosphido- and diphosphane-bridged analogues have been characterized: a) M. E. García, V. Riera, M. T. Rueda, M. A. Ruiz, M. Lanfranchi, A. Tiripicchio, *J. Am. Chem. Soc.* **1999**, *121*, 4060 – 4061; b) C. M. Alvarez, M. E. García, M. T. Rueda, M. A. Ruiz, D. Sáez, N. G. Connelly, *Organometallics* **2005**, *24*, 650 – 658; c) M. A. Alvarez, Y. Anaya, M. E. García, M. A. Ruiz, *Organometallics* **2004**, *23*, 3950 – 3962; d) M. A. Alvarez, Y. Anaya, M. E. García, V. Riera, M. A. Ruiz, J. Vaissermann, *Organometallics* **2003**, *22*, 456 – 463; e) R. L. Keiter, E. A. Keiter, M. S. Rust, D. R. Miller, E. O. Sherman, D. E. Cooper, *Organometallics* **1992**, *11*, 487 – 489.
[13] The diamagnetic dimers **1** and **2** were synthesized by H atom abstraction from $[CpM(CO)_2(PMe_3)H]$ (see the Supporting Information).
[14] W. E. Geiger, F. Barrière, *Acc. Chem. Res.* **2010**, *43*, 1030 – 1039.
[15] The $B(C_6F_5)_4^-$ salt is the most convenient because of its good solubility in CH_2Cl_2 (see also Ref. [14]). Initial results suggest that $[\mathbf{1}^{\bullet+}]PF_6^-$ and $[\mathbf{1}^{\bullet+}]BF_4^-$ may also be prepared, but their extremely low solubility thwarts solution characterization.
[16] CCDC 878972 (**1**) and 878973 ($[\mathbf{1}^{\bullet+}]B(C_6F_5)_4^- \cdot {}^1/_2\, CH_2Cl_2$) contain the supplementary crystallographic data for this paper. These data can be obtained free of charge from The Cambridge Crystallographic Data Centre via www.ccdc.cam.ac.uk/data_request/cif.
[17] R. H. Crabtree, M. Lavin, *Inorg. Chem.* **1986**, *25*, 805 – 812.
[18] Similar Mo–Mo bond contractions of about 0.2–0.3 Å seem to occur in isoelectronic—yet bridged—Mo dimers (see Ref. [12c]).
[19] This discussion pertains to the C_{2h}-symmetric *anti* rotamers, as drawn in Scheme 2. For all species, C_2-symmetric *gauche* rotamers are also observed in solution; see: R. D. Adams, F. A. Cotton, *Inorg. Chim. Acta* **1973**, *7*, 153 – 156.
[20] Because only one band is observed for $\mathbf{1}^{\bullet+}$ (see text), its average $\tilde{\nu}_{CO}$ cannot be determined.
[21] C. G. Atwood, W. E. Geiger, *J. Am. Chem. Soc.* **2000**, *122*, 5477 – 5485.
[22] M. S. Wrighton, D. S. Ginley, *J. Am. Chem. Soc.* **1975**, *97*, 4246 – 4251.
[23] C. Creutz, *Prog. Inorg. Chem.* **1983**, *30*, 1 – 73.
[24] J. P. Perdew, K. Burke, M. Ernzerhof, *Phys. Rev. Lett.* **1996**, *77*, 3865 – 3868.
[25] a) G. te Velde, F. M. Bickelhaupt, E. J. Baerends, C. Fonseca Guerra, S. J. A. van Gisbergen, J. G. Snijders, T. Ziegler, *J. Comput. Chem.* **2001**, *22*, 931 – 967; b) C. Fonseca Guerra, J. G. Snijders, G. te Velde, E. J. Baerends, *Theor. Chem. Acc.* **1998**, *99*, 391 – 403; c) ADF2010, SCM, Theoretical Chemistry, Vrije Universiteit, Amsterdam, The Netherlands.
[26] E. van Lenthe, E. J. Baerends, *J. Comput. Chem.* **2003**, *24*, 1142 – 1156.
[27] E. van Lenthe, E. J. Baerends, J. G. Snijders, *J. Chem. Phys.* **1993**, *99*, 4597 – 4610.
[28] E. K. U. Gross, J. F. Dobson, M. Petersilka, *Top. Curr. Chem.* **1996**, *181*, 81 – 172.
[29] a) E. van Lenthe, P. E. S. Wormer, A. van der Avoird, *J. Chem. Phys.* **1997**, *107*, 2488 – 2498; b) J. Autschbach, B. Pritchard, *Theor. Chem. Acc.* **2011**, *129*, 453 – 466.

